We are IntechOpen, the world's leading publisher of Open Access books Built by scientists, for scientists

4,800
Open access books available

122,000
International authors and editors

135M
Downloads

Our authors are among the

154
Countries delivered to

TOP 1%
most cited scientists

12.2%
Contributors from top 500 universities

CLARIVATE ANALYTICS BOOK CITATION INDEX INDEXED

WEB OF SCIENCE™

Selection of our books indexed in the Book Citation Index in Web of Science™ Core Collection (BKCI)

Interested in publishing with us?
Contact book.department@intechopen.com

Numbers displayed above are based on latest data collected.
For more information visit www.intechopen.com

28

Highly Defined Whale Group Tracking by Passive Acoustic Stochastic Matched Filter

Frédéric Bénard[1], Hervé Glotin[2] and Pascale Giraudet[3]
[1,2]*Systems & Information Sciences Laboratory (LSIS - UMR 6168 USTV&CNRS), Université du Sud-Toulon-Var*
[3]*Department of Biology, Université du Sud-Toulon-Var*
France

1. Introduction

In this paper, we compare two low cost time-domain tracking algorithms based on passive acoustics. The problem consists in tracking an unknown number of sperm whales (Physeter catodon). Clicks are recorded on two datasets of 20 and 25 minutes on an open-ocean widely-spaced bottom-mounted hydrophone array. The output of the method is the track(s) of the Marine Mammal(s) (MM) in 3D space and time. Firstly, we briefly review studies of the Stochastic Matched Filter (SMF) detector and its performances with a reflected click cancellation, the Teager-Kaiser-Mallat (TKM) filtering, the source separation methods and the main characteristics of MM signals. Then, we propose a real-time algorithm for MM transient call localization. We also recall the Cramér-Rao Lower Bound (CRLB) Kay (1993) and the confidence ellipses theory to predict the reachable accuracy and compare it to the tracking results. In Section 3 we show and compare results of track estimates with results from specialized teams and compare SMF versus TKM localization. Then, the system is evaluated with the confidence ellipses on the trajectories. Finally, we discuss on the possible dynamic behavior of the whale that these localizations offer, like hunting and foraging strategies.
This paper deals with the 3D tracking of MM using a widely-spaced bottom-mounted hydrophone array in deep water. It focuses on sperm whale clicks. There were previous algorithms developed in the state of the art Giraudet & Glotin (2006a;b); Morrissey et al. (2006); Nosal & Frazer (2006) but none of them has satisfying results for multiple tracks and most of them are far from being real-time. Our main goal is to build a robust and real-time tracking model, despite ocean noise, multiple reflected clicks, imprecise sound speed profiles, an unknown number of MM, and the non-linear time-frequency structure of most MM signals. Background ocean noise results from the addition of several noises: sea state, biological noises, ship noise and molecular turbulence. Propagation characteristics from an acoustic source to an array of hydrophones include multipath effects (and reverberations, Fig. 1), which create secondary peaks in the Cross-Correlation (CC) function that the generalized CC methods cannot eliminate. In Caudal & Glotin (2008b); Glotin et al. (2008), we gave an extension of Giraudet & Glotin (2006b) that shows multiple tracking using TKM. Here we improve this model using SMF which also allows an efficient Inter-Click-Interval and reflected click removal process.

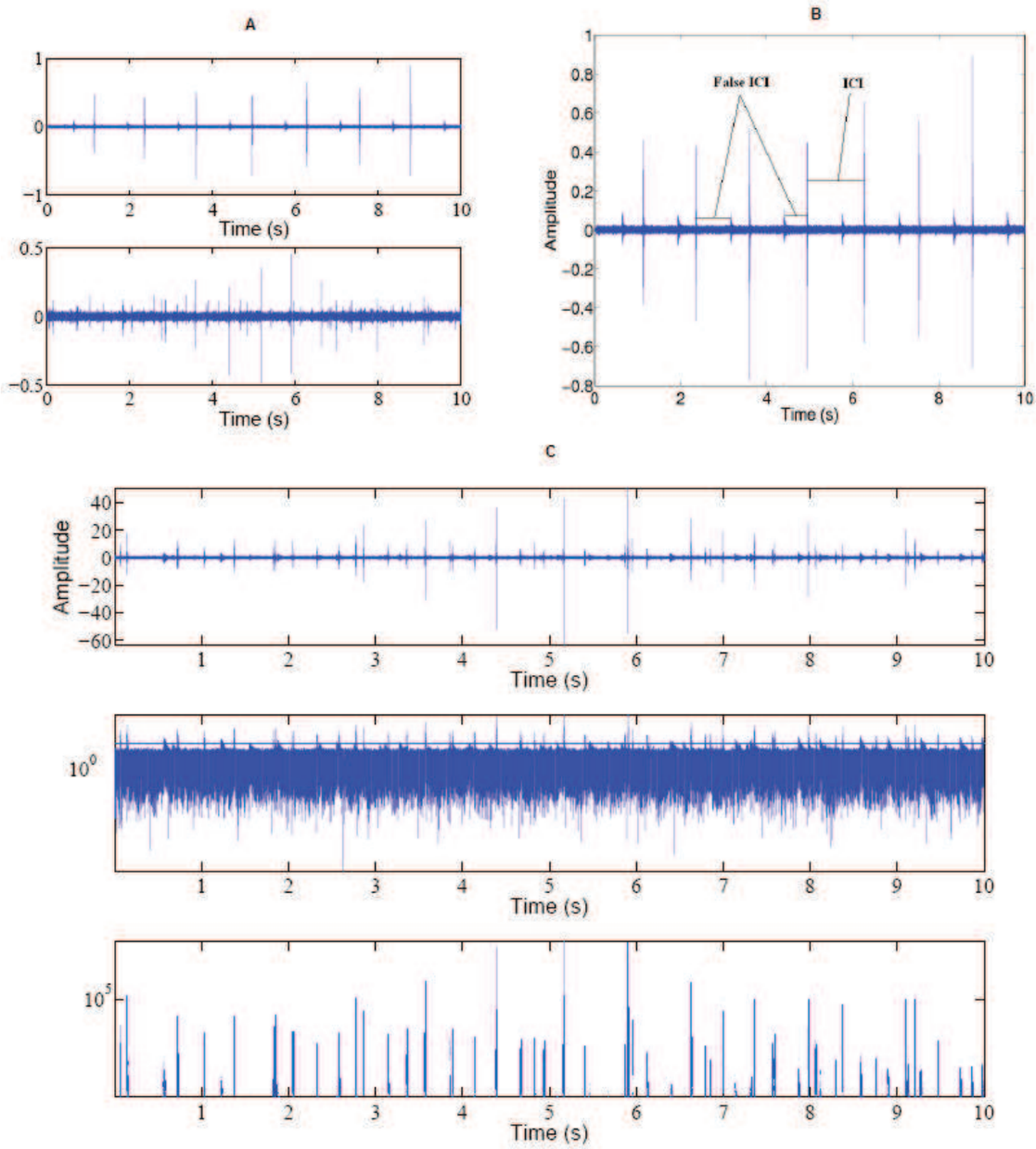

Fig. 1. (A): on the top, a raw signal from dataset2 (D2) and hydrophone 7 (H7) during the first 10 s of recording, containing 7 clicks and their reflected click. At the bottom, 10 s from dataset 1 (D1), hydrophone 1 (H1) containing several (4) simultaneous emitting whale clicks and the reflected clicks. (B): a click train with reflected click from a single sperm whale. We can see an Inter-Click-Interval (ICI), and two false ICI between direct and reflected clicks. (C): Example of a raw multipe whales' signal on H1 (10 s) (top) and the corresponding $\Lambda(x)$ presented in paragraph 3.2 with the threshold in a log-scale (middle) and the thresholded signal (bottom).

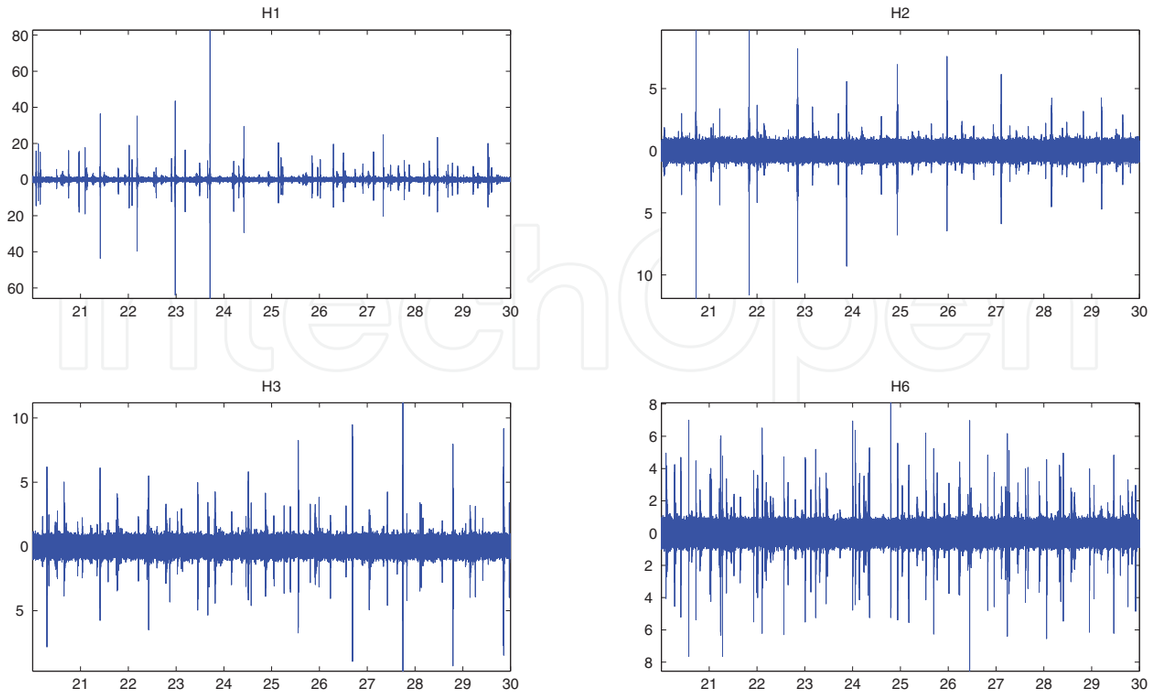

Fig. 2. H1 to H6: plots of a 10 sec samples of raw signals from the four hydrophones of the dataset D1 (time in sec).

2. Hydrophone array characteristics

2.1 Records Settings

D	Hydro	Dist (m)	X (m)	Y (m)	Z (m)
D1	H 1	5428	18501	9494	-1687
	H 2	4620	10447	4244	-1677
	H 3	2514	14119	3034	-1627
	H 4	1536	16179	6294	-1672
	H 5	3126	12557	7471	-1670
	H 6	4423	17691	1975	-1633
D2	H 7	1518	10658	-14953	-1530
	H 8	4314	12788	-11897	-1556
	H 9	2632	14318	-16189	-1553
	H 10	3619	8672	-18064	-1361
	H 11	3186	12007	-19238	-1522

Table 1. Hydrophones positions: Dist=Distance to the barycenter of the set. (H4 and H5 are out of order)

The signals are records of March 2002 from the ocean floor (about 1500 m) near Andros Island - Bahamas (Tab.1), provided with celerity profiles. Datasets are sampled at 48 kHz and contain MM clicks and whistles, background noises like distant engine boat noises. Dataset1 (D1) is recorded on hydrophones 1 to 6 during 20 min (see Fig.2 for a sample view) while the dataset 2 (D2) is recorded on hydrophones 7 to 11 with 25 min length. We will use a constant sound speed with $c = 1500ms^{-1}$ or a linear profile with $c(z) = c_0 + gz$, where z is the depth,

$c_0 = 1542ms^{-1}$ is the sound speed at the surface and $g = 0.051s^{-1}$ is the gradient Caudal & Glotin (2008b). Sound source tracking is performed by continuous localization in 3D using Time Delays Of Arrival (TDOA) estimation from four hydrophones (Tab.1).

2.2 Cramér-Rao lower bound from the hydrophone array geometry

For each hydrophones array, the Cramér-Rao Lower Bound (CRLB) provides the maximum accuracy for the estimation of any source position. Considering a constant sound speed profile, the function model of the Time Delay Of Arrival (TDOA) is defined by:

$$s(\theta) = \frac{1}{c_s}\left[||X_i - \theta|| - ||X_j - \theta||,\ ||X_i - \theta|| - ||X_k - \theta||,\ ||X_i - \theta|| - ||X_l - \theta||\right]^T, \quad (1)$$

where $||\ ||$ denotes the euclidian norm, X_i is the hydrophone i vector coordinate, θ is the unknown parameters vector $[x\ y\ z]^T$ and c_s the celerity. Here $i = 1$, $j = 2$, $k = 3$, $l = 4$. Thus, considering the TDOA noise as a Gaussian process and B its variance-covariance matrix, the Fisher Information matrix is:

$$I_\theta = \nabla_\theta s(\theta) B^{-1} \nabla_\theta^T s(\theta). \quad (2)$$

Then, the CRLB is $B_\theta = I_\theta^{-1}$. The solution error ellipses are contours of constant value of the inner product $\theta I \theta$.
We compute the CRLB (in meter) in the space (x,y,z) and plot the values for both datasets (Fig.3). We consider that the standard deviation of the noise is equal to the quantification noise with a sampling frequency of 480 Hz. The main dependencies of the bounds are the noise and the array configuration. In figures 3.A to F, the CRLB on y and z is shown for a depth of 500 m, and is just about the same for a depth of 1000 m as shown in figures 3.G-H.

3. Filters design

3.1 Teager-Kaiser-Mallat filtering

A sperm whale click is a transient increase of signal energy lasting about 20 ms (Fig.1). Therefore, we use the Teager-Kaiser (TK) energy operator Kandia & Stylianou (2006) on the discrete data:

$$\Psi[x(n)] = x^2(n) - x(n+1)x(n-1), \quad (3)$$

where n denotes the sample number. Considering the raw signal $s(n)$ (sample n of the raw signal) as:

$$s(n) = x(n) + u(n), \quad (4)$$

where $x(n)$ is the signal of interest (click), $u(n)$ is an additive noise defined as a process realization considered Wide Sense Stationary (WSS) Gaussian during a short time. By applying TK to $s(n)$, $\Psi[s(n)]$ is:

$$\Psi[s(n)] \approx \Psi[x(n)] + w(n), \quad (5)$$

where $w(n)$ is a random gaussian process Kandia & Stylianou (2006). The output is dominated by the clicks energy. Then, we reduce the sampling frequency to 480 Hz by the mean of 100 adjacent bins to reduce the variance of the noise. We apply the Mallat's algorithm

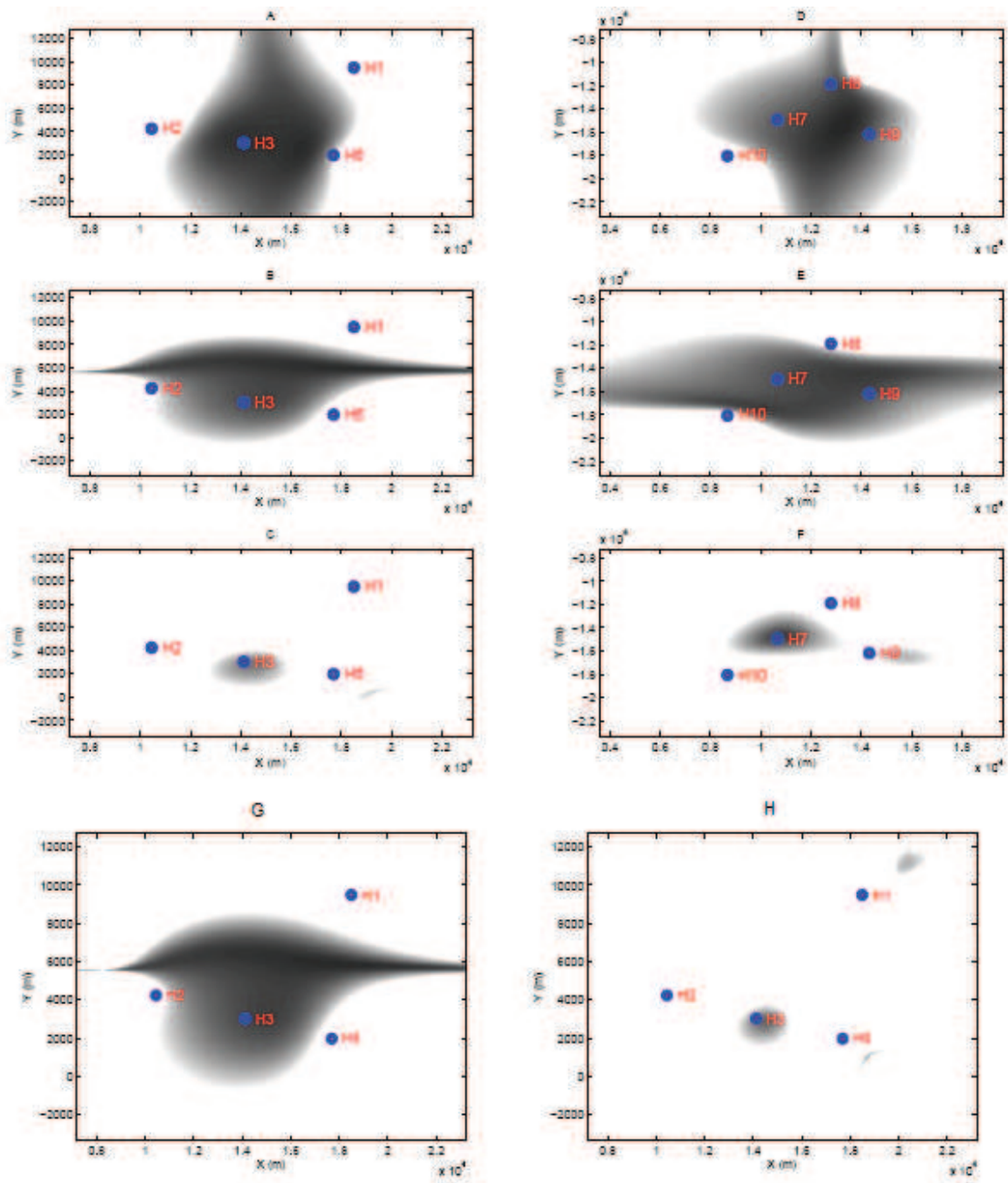

Fig. 3. CRLB values scaled in gray colors with a plan view: black means a null CRLB and white a CRLB≥10 m. For the figures A to F, a depth of 500 m was chosen. (A): CRLB on x values, dataset D1. (B): y, D1. (C): z, D1. (D): x, D2. (E): y, D2. (F): z, D2. (G): CRLB on y axis, plan view, dataset D1, depth=1000 m. (H): CRLB on z axis, plan view, dataset D1, depth=1000 m.

Mallat (1989) with the Daubechies wavelet Adam et al. (2005) (order 3) into the process. The signal is denoised by a universal thresholdingDonoho (1995). This filtering step is very fast and without any parameter. The Fig.5-b shows the filtered signal of multiple emitting MM (Fig.5-a). The click detection Kandia & Stylianou (2006) is not a concern. The purpose is to ameliorate the TDOA estimation, but the reflected clicks are not removed. The TK operator can be used for detection but need an empirical threshold, thus we need a more adaptive method. The purpose of this paper is not a full comparison between the performances of two detectors, but to offer two methods for the whale tracking and the performance relative to these methods.

3.2 The Stochastic Matched Filter

The SMF, which is a filtering method, is employed here for detection. The clicks and sea noise are considered as gaussian stochastic process with 0-mean. Considering a stochastic process s (of length N), the covariance matrix is $E(ss^T) = A$. We also consider an additive, centered and independent noise b with the variance-covariance matrix B. Those processes are not correlated to each other and the matrices are supposed positive and full rank. The SMF theory Courmontagne & Chaillan (2006); Juennard (2007) says that the linear filter h of length N that maximizes the Signal to Noise Ratio (SNR) is the eigen vector solution of:

$$Bh = \lambda Ah, \tag{6}$$

associated to the greatest eigen value λ_0. Thus, we are looking for the eigen values and vectors of $B^{-1}A$. The function used for the detection is:

$$\Lambda(x) = [h^T x]^2, \tag{7}$$

with x a N-length window. Denoting ρ as the SNR gain after filtering, and $\tilde{M}$ a matrix normalized by its trace, we have $\rho = \frac{h^T \tilde{A} h}{h^T \tilde{B} h}$. We work on windows of 20 ms which correspond to a click mean length. A is computed with an average of 1000 sperm whale clicks, and B is calculated directly from the hydrophone signals. After h is calculated for each channel, we are able to filter the signal with one bin of shifting. Thus, we obtain $\Lambda(x)$ (Fig.1.C) with a threshold chosen considering the performance that maximizes the synthetic Receiver Operating Characteristic (ROC).

We compute the ROC for a SNR of -10 dB which corresponds to an emitting whale at about 5 km from the receptor. SNR (dB) is computed with $10log_{10}(\frac{P_s}{P_b})$ with $P_s = \frac{s^T s}{N}$ and $P_b = E(\frac{b^T b}{N})$. The detection rate for 1% false alarm rate of the SMF is 49%. To the contrary of the TKM filter, as we use SMF as a detector, we have a date for each probable click, and thus we can eliminate false detections like reflected clicks.

3.3 Reflected click cancellation

In order to generate robust estimates of the TDOA we avoid relying completely on correlation based techniques. In reality, the SMF detector often detects the reflected clicks present after each click (Fig.1.B). To remove them, we work on each detection date given by the SMF in a channel, considering it as a reflected click or a click, and we discriminate the direct paths and the reflected arrivals. Since the multi-path arrivals pass through the surface layer and are reflected from the sea air interface, they are subject to significant surface reverberation. This causes a temporal elongation (Fig.4.C, White et al. (2006)). Dan Ellis and al. Halkias & Ellis (2006) proposed a cancellation method based on frequential propreties. Here we propose for a

simpler temporal discrimination. Therefore, on the raw signal, we smooth each potential click and calculate the sum of the normalized envelope (Fig.4.D). Consequently, the results from direct and reflected paths are significantly different.
A relatively crude threshold allows one to distinguish the majority of reflected signals from the direct arrivals. There is no demand for highly accurate discrimination; subsequent Giraudet & Glotin (2006b) delay estimation algorithm performs well as long as the majority of events surviving discrimination correspond to direct arrivals.

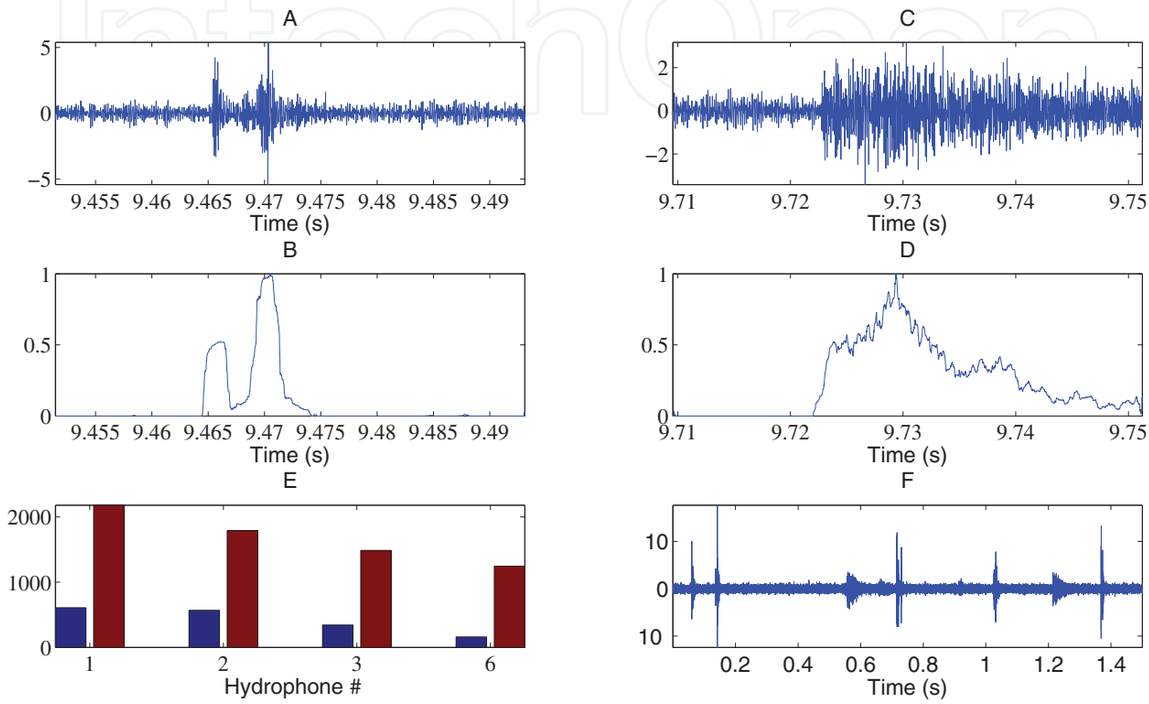

Fig. 4. A direct click (A) with its absolute normalized smoothed envelope (B) compared to a reflected click (C) and its envelope (D). (E): number of reflected clicks (bar on the left) and clicks (bar on the right) detected for each hydrophone in D1 (H4 and H5 are out of order). (F): Raw signal (H1) showing clicks and reflected clicks with several emitting whales.

hydrophone #	7	8	9	10	11
Reflected clicks detected	602	488	473	467	439
Clicks detected	1355	1232	1147	1058	1032
Real number of clicks	1378	1378	1378	1378	1378

Table 2. SMF + reflected click cancellation statistics for dataset 2.

hydrophone #	1	2	3	6
Reflected clicks detected	609	481	245	176
Clicks detected	2129	1894	1461	1293

Table 3. SMF + reflected click cancellation statistics for dataset 1. We do not know yet the exact number of clicks in D1.

The Tab.2-3 summarizes the reflected clicks and clicks detected in both datasets. All clicks in D2 are manually detected. We see that the number of clicks detected with the SMF is varying

with the hydrophone because of the different SNR on each hydrophone, and that the reflected clicks are partly rejected (considering one reflected click per click).

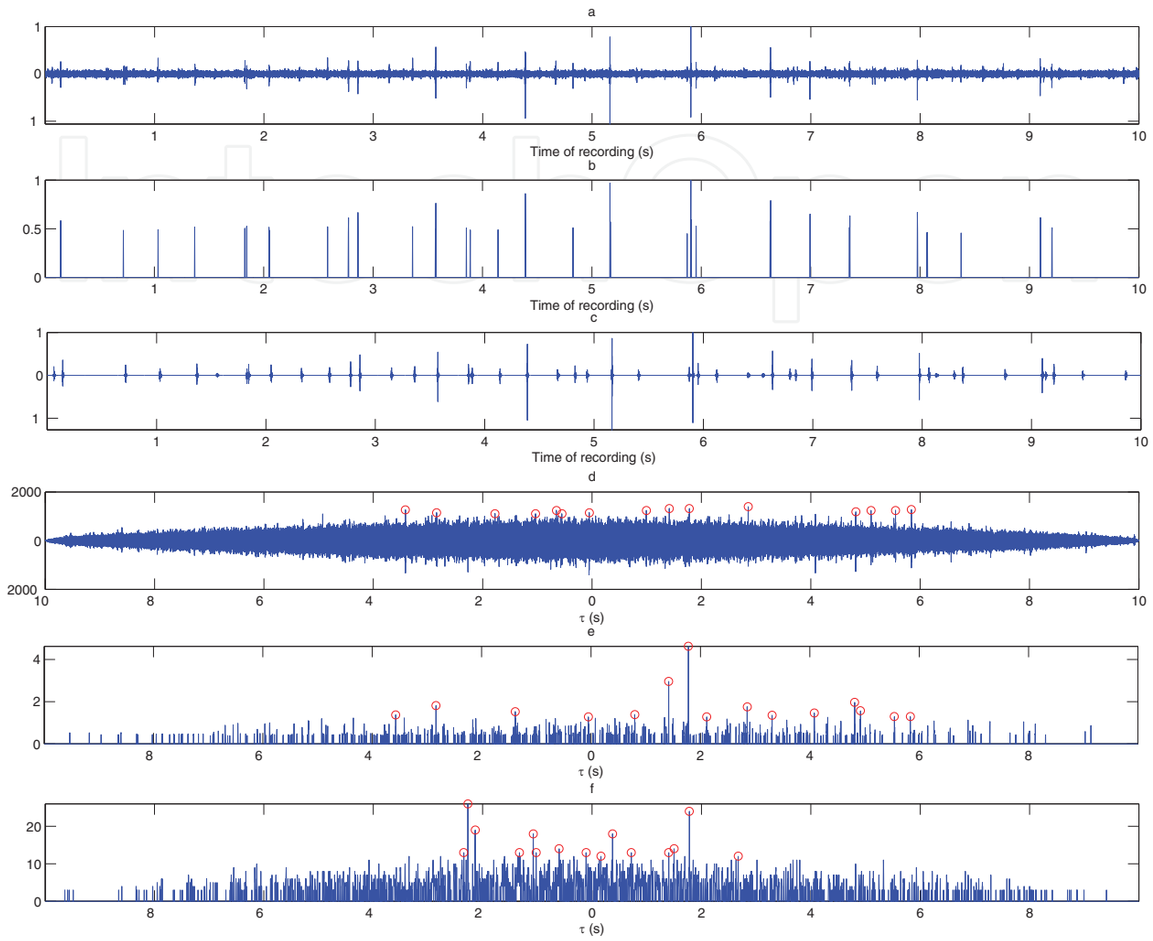

Fig. 5. (a): raw signal for dataset D1 of H1 during the first 10s of recording showing multiple emissions. (b): (a) after TKM filtering. (c): (a) after the SMF. (d): CC between (a) and corresponding raw signal chunk of H3. (e): idem than (d) but with (b). (f): idem than (d) but with (c). Circles on the top of some peaks correspond to the 15 maximum peaks (that are used for localization).

4. Robust and Fast localization method

4.1 Rough TDOA estimation and selection

Either after TKM or after [SMF + reflected click cancellation], we process rough TDOA estimation and selection. The Fig.5-a,c are respectively a raw multiple emitting MM signal, and the corresponding complete filtered signal. First, TDOA estimates are based on MM click realignment only. Every 10 s, and for each pair of hydrophones (i, j), the difference between times t_i and t_j of the arrival of a click train on hydrophones i and j is referred as $T(i, j) = t_j - t_i$. Its estimate $\widetilde{T}(i, j)$ is calculated Giraudet & Glotin (2006a;b) by CC of 10 s chunks (2 s shifting) of the filtered signal for hydrophones i and j. We keep the 15 highest peaks on each CC to determine the corresponding $\widetilde{T}(i, j)$. The filtered signals give a very

fast rough estimate of TDOA (precision $\pm$ 2 ms). The Fig.5.d shows the CC with the raw signal, and the Fig.5.e,f with respectively the TKM filtered signal and the SMF. The number of common peaks between TKM, SMF and raw filtering methods are in Tab.4. At most, only 23% of the TDOA are common between the 2 filters, the 23% corresponding to the TDOA of the high SNR clicks. Without any filtering, CC generates spurious delays estimates and the tracks are not correct. Finally, thanks to the $\widetilde{T}$ transitivity constrained system described in Giraudet & Glotin (2006b), we keep $\widetilde{T}$ triplets coming from the same source.

4.2 Localization with a constant and a linear profile

Thanks to the measured delays and an acoustic model based on a constant or a linear sound speed profile, the least squares cost function determines the MM positions using a multiple non-linear regression with the Gauss-Newton method Giraudet & Glotin (2006b) (Levenberg-Marquardt technique Marquardt (1963)). The residuals are approximatively following a Chi-square distribution with $Nc - d$ degrees of freedom, which is noted X^2_{Nc-d}, where Nc is the number of hydrophones couples considered and d the number of unknowns, that are the coordinates (x, y, z). The position is accepted if the residual is inferior to a threshold x, that is calculated solving $P = prob(X^2_{Nc-d} > x)$ with $P = 0.01$ (we keep 99% of the estimates).

5. Results

5.1 Tracking comparisons

In this section, we give the tracks results for TKM and SMF for D1 and D2 dataset. For the dataset D2 (Fig.6), a constant and a linear sound speed profile were used like in Caudal & Glotin (2008b) and the results are similar to those of Morrissey's Morrissey et al. (2006) and Nosal's Nosal & Frazer (2006) methods. The diving profile underlines a bias of about -70 m between the linear and the constant profiles results, emphasizing the importance of the chosen profiles. Moreover with the linear sound speed, the results are about the same as those of Morrissey and Nosal, who used profiles corresponding to the period and place of the recordings. The results on D1 are shown in Fig.7,8,9, and are for a linear sound speed profile. The TKM method lets appear an artifact whale (yielding to 5 whales), which is due to the reflected clicks produced by the whale with the (+) symbol which are eliminated thanks to the reflected click removal with the SMF method (without the reflected click removal, the same virtual whale appears in the SMF results) but we can not apply a reflected click removal on TKM because it is not used as a detector. We thus localize 4 MM with the SMF method. The number of positions estimated for each method is in Tab.4. The confidence regions are computed for both datasets with a Monte Carlo method. The ellipses maxima (30 m) fit with MM length (20 m), which is acceptable.

In the SMF method, there are much more estimated positions because the SMF, detects partically all the clicks and even the ones with a bad SNR. This last method depends on the direction and the distance of the whale to the hydrophone. The signals correlation for the TDOA estimation are thus binary, and do not contain the information of distance, whereas the Teager-Kaiser method just enhances the correlation, where the signal is filtered without detection and thus low click energy results in small correlation, compared with the high click correlation. This is why in the 3D region, when the whale is in the opposite direction and/or emits small energy clicks, the SMF method returns more positions. The result for the left whale (represented with '+' in Fig. 7) in the multiple whales case is a good illustration. In the first trajectory part, the whale is off-axis with all the hydrophones, so the SNR is low on pratically

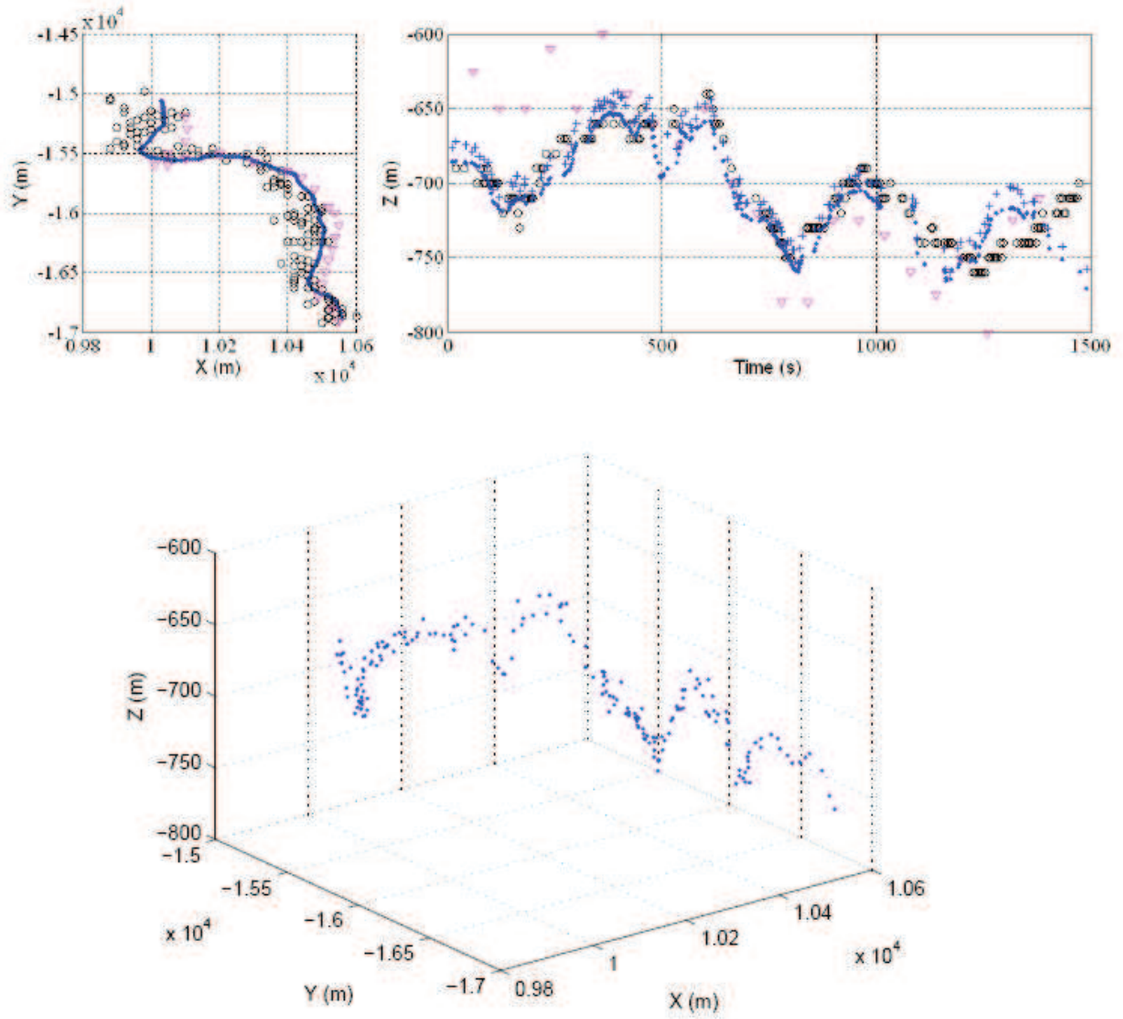

Fig. 6. Top: plan view and diving profile of the MM in D2, our estimates with a linear profile and the SMF method (.) or TKM (+); and estimates of Morrissey's ($\triangledown$) and Nosal's methods (o). The results with a constant profile underline a bias of about -70 m Caudal & Glotin (2008b). Bottom: 3D plot of the trajectory in D2.

all the hydrophones, and thus, TDOA extraction and localization are difficult with the TKM method (SMF is much better). In the last part, the whale is on-axis with 2-3 hydrophones, then the TDOA and positions estimation are facilitated thanks to the high SNR and then the TKM method generates more positions per time sample relatively to the first trajectory part.
To summarize the confrontation, SMF produces more positions than TKM because it is a more efficient detector. But it does not modify the accuracy of the position estimation, as shown below in section 5.2.

5.2 Confidence region analyses

To compute the ellipses, we apply a Monte Carlo method and a gaussian distribution noise with the standard deviation described above. For each $\widetilde{T}$ realization, the source position is calculated. We deduce the variance and the mean for each position to plot the confidence

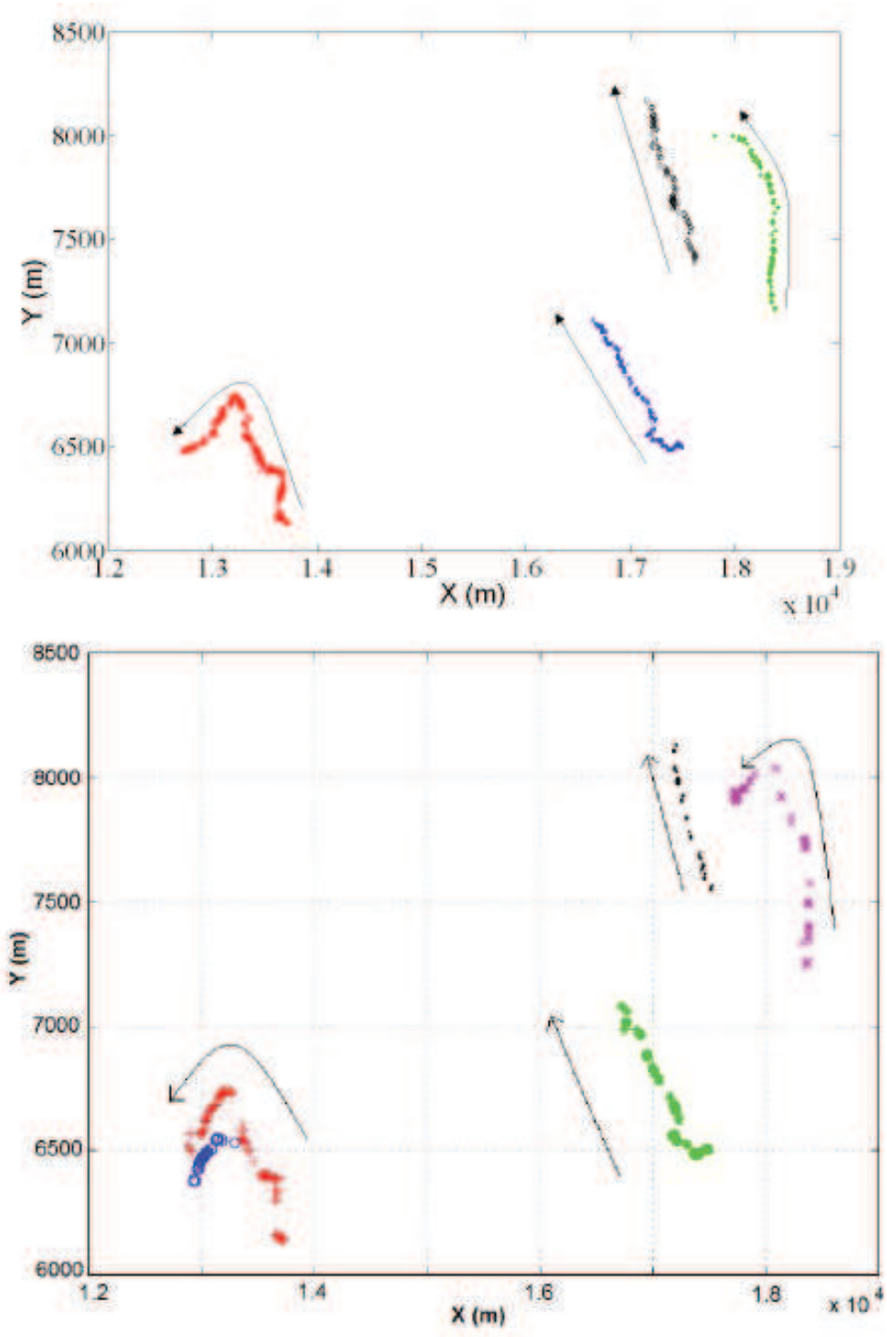

Fig. 7. On the top, plan view of several whale tracks in D1 with the SMF method. Each symbol corresponds to one of the 4 whales. The arrows show the directions. On the bottom, plan view in D1 with the TKM method. Each symbol corresponds to one of the 5 whales. Compared to the SMF, one false whale appears due to the lack of reflected click removal for TKM. Another great difference is the high definition of the SMF track compared to TKM ones, as discribed in Tab.4. A 3D plot of the trajectores with the SMF method can be seen on Fig.8.

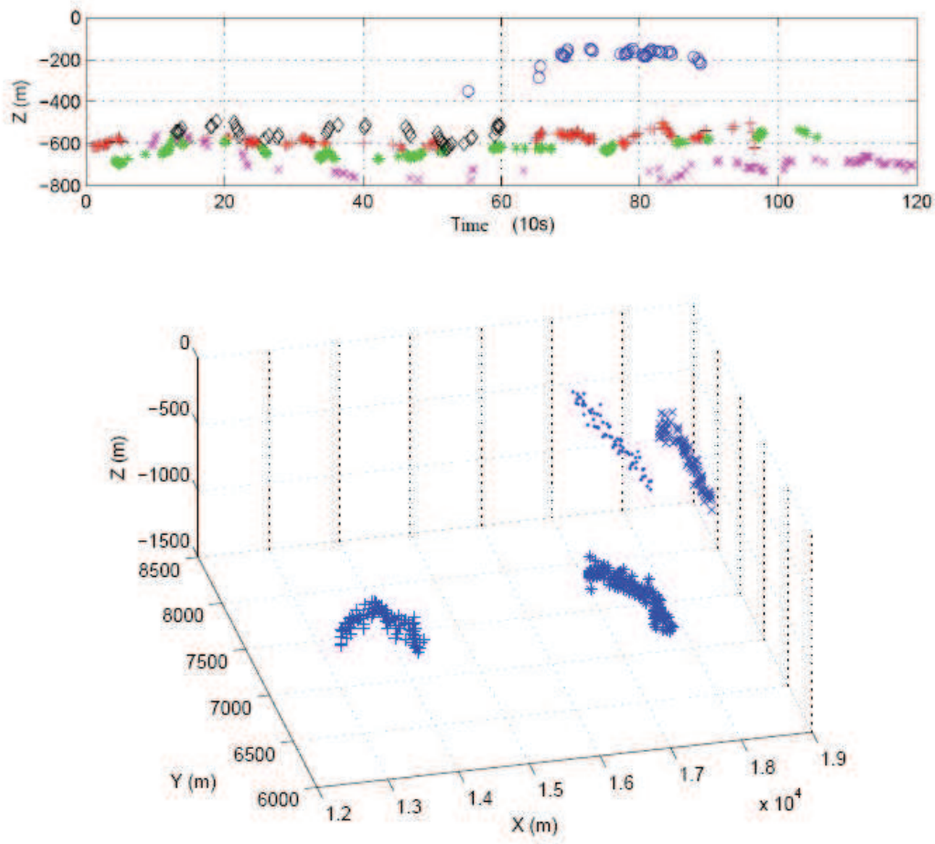

Fig. 8. Top: averaged diving profile in D1 with TKM method. Each symbol corresponds to one whale in Fig.7 ((+), (o), (hexagon), (diamond)). The SMF results in section 5.2 demonstrate that the 'o' is a reflected click of the '+' whale (cf Fig.7). Bottom: 3D plot of the trajectories in D1.

% of common TDOA	Raw	TKM	SMF
Raw	5/13	3%	2%
TKM	12%	103/57	14%
SMF	10%	23%	387/143

Table 4. In diagonal, the number of positions obtained in D1/D2. Above the diagonal of this table, we give the % of common TDOA in D1, and under it, the % of common TDOA in D2.

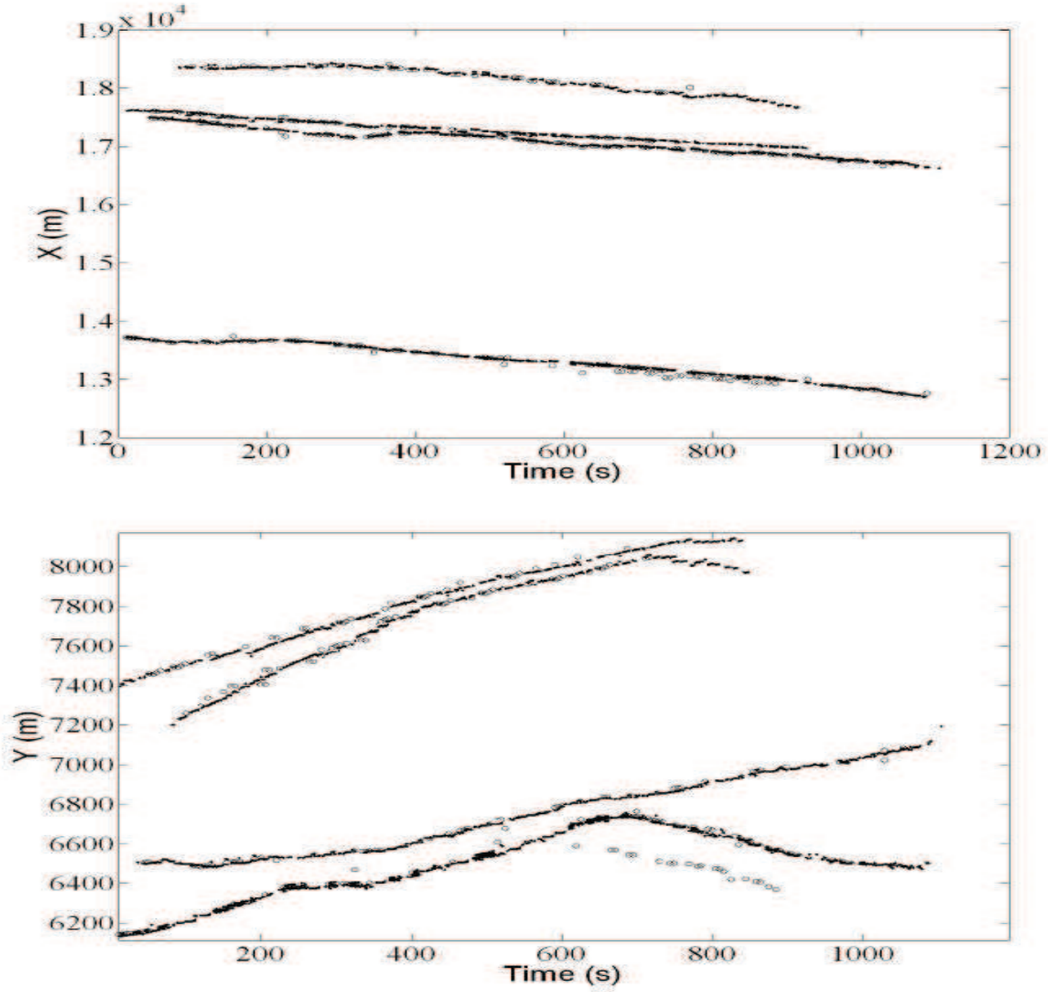

Fig. 9. Comparisons between SMF tracks (.) and TKM tracks (o) in D1, demonstrating that SFM outperforms TKM. X(t) (Y(t)) coordinates are on the top (bottom). We can see that the number of positions is far larger with the SMF than TKM (see Tab.4).

regions with a confidence level of 0.95, which means that there is 0.95 probability for the whale to be in the ellipse centered on the position. In dataset D2, the mean values of the confidence intervals on X, Y, Z axes are about 18, 16 and 30 m (Fig.10). The results confirm that the errors on the vertical axis are meaningfully higher than the other axes because the distance between each hydrophones in this direction is smaller (the maximum difference on the Z axis between hydrophones is 200 m). As estimated by the CRLB analysis in section 2.2, the farthest whales in dataset D1 from the hydrophones array center have a larger uncertainty with an error of about 20 to 30 m on X and Y axes (Fig.10), while the whales close to the center (Fig.10) exhibit an error of about 10 to 20 m like for D2 (Fig.7). These uncertainties are reasonable according to the sperm whale length (20 to 30 meters).

Comparing the CRLB with the ellipses, we can see the correlation between maximum accuracy and confidence regions. Figures 3-C and 3-F show the accuracy on z axis is larger than 10 m

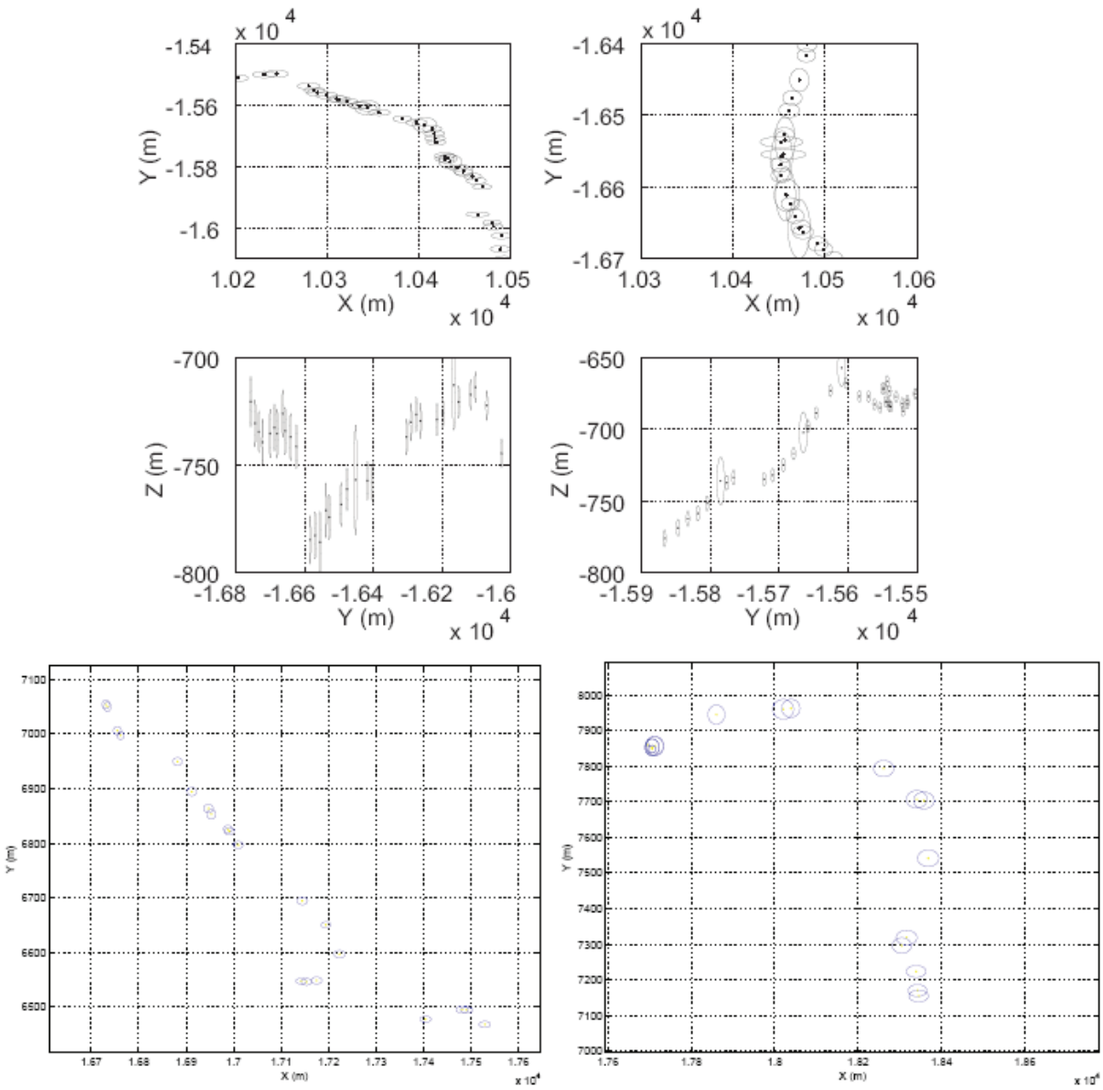

Fig. 10. Top: confidence region projection on (X,Y) and (Z,Y) axes for different trajectories in D2 with the SMF. Bottom left: confidence region projection on X and Y for the whale in the middle ('*' symbol in Fig.7), D1 dataset, trajectory with the SMF. Bottom right: confidence region projection on X and Y for the whale in the right (x symbol), D1 dataset, trajectory with the SMF.

for both datasets in the tracking regions, which is consistent with the ellipses results, but in the case of D1, the diving profile estimation is not suitable, mainly due to the z-component of the CRLB (Fig.3.H). The CRLB (in D1, Fig.3.D-E) also explains that the farthest whale has larger confidence regions. But for both datasets, the CRLB on x and y is far inferior to 10 m inside the array whereas our ellipses are about 10 to 20 m, which is maybe caused by other parameters involved in, like the approximated celerity profile.

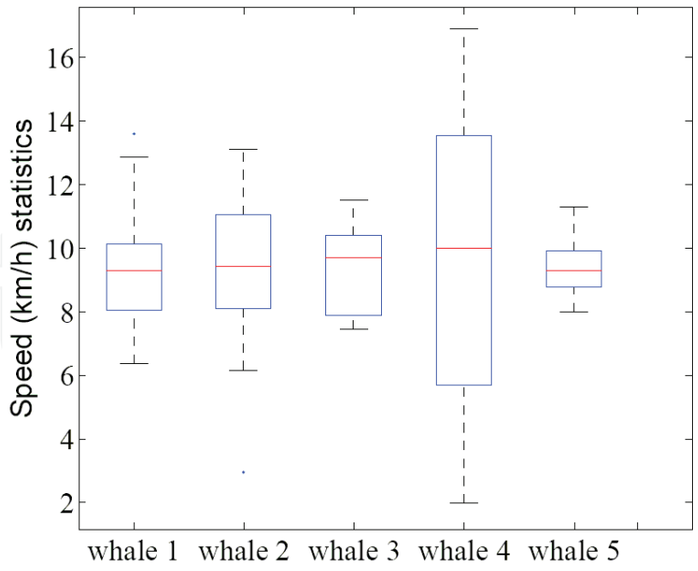

Fig. 11. Speed (averaged on 30 s windows) statistics on the whole set for each whale in dataset D1 (whales 1 to 4, numeroted from left to right) and dataset D2 (whale 5). The central line of the box is the median of speed and the lower and higher lines are the quartiles. The whiskers show the extent of the speed (the average speed is about 9 km/h, likely as regular sperm whale).

6. Perspectives on whale behavior analyses

Our method gives a real-time multi tracks of a whale group. The Fig.11 shows the speed profile for each whale. These localizations allow to use the true TDOA and to label the signal. This leads to a precise Inter-Click-Interval (ICI) extraction Caudal & Glotin (2008a). Other features can also be extracted thanks to this localization, such as the whale speed, the energy of each click, distance to a given hydrophone and head's angles with a given hydrophone. These features would give some relevant informations on the whale's behavior when hunting prey at depth. It is admitted that sperm whales make a slow pitch movement and created a faster pitch or yaw movement in synchronization with the clicking activity. The literature Laplanche et al. (2005),Laplanche et al. (2006) suggested that sperm whales would, at depth, make an asymmetric scan of the surrounding water and that during the search phase, sperm whales would methodically scan a cone-shaped mass of water when searching for prey. This scan would suggest that each sperm whale click is generated to aim in a specific direction and at a specific range. Sperm whales would move physically to change the click beam direction, and control level and ICI to change the click target range. Authors in Laplanche et al. (2005) then pointed out a correlation between click level variations and ICI. The hypothesis explaining such a correlation would be click level control: sperm whales would click slowly at a high source level and faster at a lower source level. We are currently analysing the dependencies of all these results that will validate or note this model.
The Fig.12 summarizes different possible features computation in our framework, and their connections with our tracking algorithm. Actually, these measurements are correlated with each other and offer a new large research field for whale behavior analysis.

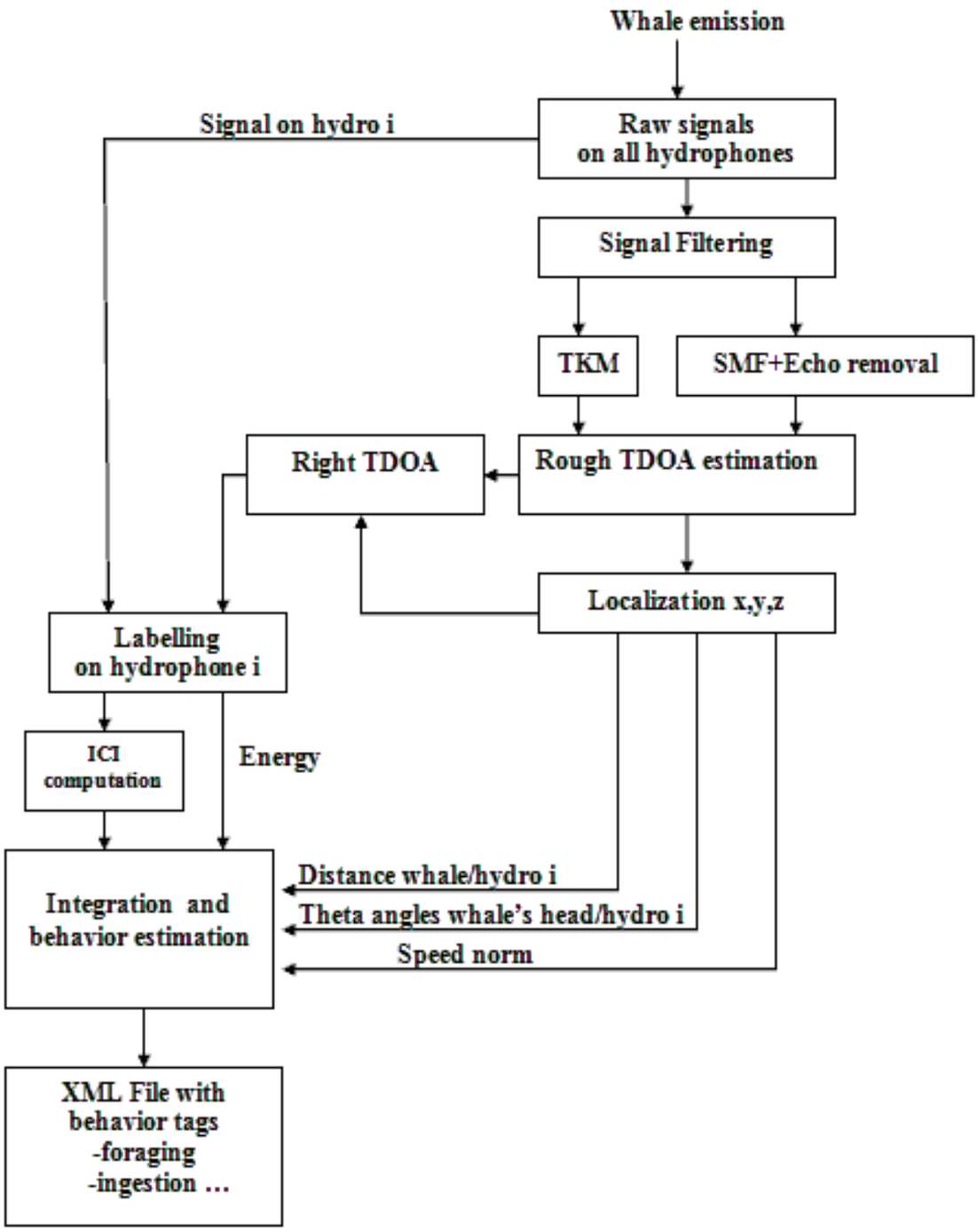

Fig. 12. Block scheme of the possible features extraction.

7. Conclusion

We present in this paper a method using a real-time algorithm for tracking one or multiple emitting sperm whales, in order to analyse whale behavior and to index hydrophones audio

files. All the derived features (speed, direction changes) are likely according to the cetologists knowledge. Part of the results presented in this paper are in video demonstrations on http://glotin.univ-tln.fr/PIMC/DEMO.
The localization step is run in real-time on a standard laptop, and works for one or multiple emitting sperm whales. The depth results with a constant speed contain a bias error due to the refraction of the sound paths from the MM to the receivers which a linear speed corrects. Another way to tackle the speed profile issue Glotin et al. (2008) would be to estimate it as a fourth unknown in the regression. However, SMF perfoms better than TKM method (see Tab.4, 103 positions estimated for TKM versus 387 for SMF in D1). The SMF provides a simple way for detecting the sperm whales with good performance, where all the thresholds are learned online and no parameters are needed considering the database. In D2, results indicate that only one sperm whale was emitting in the area, as also analysed by MorrisseyMorrissey et al. (2006) and NosalNosal & Frazer (2006), but not in real-time. Moreover, according to ROSA Lab estimationHalkias & Ellis (2006) based on click clustering, and also preliminary results from the SOEST (School of Ocean and Earth Science and Technology), the number of MM for each 5 min chunks on D1 (Tab.5) is similar to ours. The localization accuracy is computed via the CRLB and the confidence ellipses are correct considering the MM length. The depth error is mainly due to the low precision reachable with the CRLB considering the array configuration.
Our method allows to label the signal and then will be used to extract features presented in Fig.12. Other characteristics such as inter-pulse-interval (a click is composed of multiple pulses), which contain informations about the whale's pitch and yaw behavior. The features discussed above would allow us to analyse whale's foraging and hunting behavior with a good resolution. Finally, we can index the files thanks to the features extracted. Therefore, a XML structure can be generated and include some behavior tags for a rapid access to the acoustic data. Our method offers facilities for robust online passive acoustics behavior studying of clicking MM in open ocean. More research will be conducted to reveal high level features (ICI, behavior, hunting) from the tracks.

5 min chunks	0-5	5-10	10-15	15-20
ROSA Lab	4.3	5.3	4	3.6
PIMC TKM	4	4	4	3
SOEST	4	4	4	2
PIMC SMF	4	4	4	2

Table 5. Counting number estimations of whales in D1. First row is the five minutes chunks of D1, second is the averaged number of whales estimations from ROSA Lab, third and fifth are our estimations (PIMC TKM and SMF). The estimates of the SOEST lab Hawaii are given by personnal communication from E.M.Nosal (preliminary results from Bellop model).

8. Acknowledgments

We thank the Atlantic Undersea Test And Evaluation Center (AUTEC) and the Naval Undersea Warfare Center (NUWC) for having provided the dataset. This research was conducted within the international sea *pôle de compétitivité* at Toulon-France, through "Plateform for Integration of Multimodal Cetacean data (PIMC)". Part of this work is funded by the "Conseil régional Provence-Alpes-Côte d'Azur" France, and Chrisar Software Inc.

Another part of this work has been previously pattented[1]. We thank as well O.Adam, R.Morrissey and E.Nosal for the use of their work.

9. References

Adam, O., Lopatka, M., Laplanche, C. & Motsch, J.-F. (2005). Sperm whale signal analysis: Comparison using the autoregressive model and the wavelets transform, *International Journal of Information Technology* 2: 1–8.

Caudal, F. & Glotin, H. (2008a). Automatic inter-click-interval (ici) and behavior estimation for one emitting sperm whale., *PASSIVE 08 IEEE*.

Caudal, F. & Glotin, H. (2008b). Multiple real-time 3d tracking of simultaneous clicking whales using hydrophone array and linear sound speed profile, *ICASSP IEEE* p. 4p.

Courmontagne, P. & Chaillan, F. (2006). The adaptive stochastic matched filter for sas images denoising, *OCEAN 2006* pp. 1–6.

Donoho, D. L. (1995). De-noising by soft thresholding, *IEEE Trans. IT* 41: 613–627.

Giraudet, P. & Glotin, H. (2006a). Echo-robust and real-time 3d tracking of marine mammals using their transient calls recorded by hydrophones array, *ICASSP IEEE*.

Giraudet, P. & Glotin, H. (2006b). Real-time 3d tracking of whales by echo-robust precise tdoa estimates with a widely-spaced hydrophone array, *Applied Acoustics* 67: 1106–1117.

Glotin, H., Caudal, F. & Giraudet, P. (2008). Whales cocktail party: a real-time tracking of multiple whales, *International Journal Canadian Acoustics* 36(1): 141–147.

Halkias, X. & Ellis, D. (2006). Estimating the number of marine mammals using recordings from one microphone, *ICASSP IEEE*.

Juennard, N. (2007). *Acoustic submarine detection and localisation of very high energy particules*, Thèse de doctorat, University of Toulon.

Kandia, V. & Stylianou, Y. (2006). Detection of sperm whale clicks based on the teager-kaiser energy operator, *Applied Acoustics* 67: 1144–1163.

Kay, S. (1993). *Fundamentals of statistical signal processing*, Prentice Hall, PTR.

Laplanche, C., Adam, O., Lopatka, M. & Motsch, J.-F. (2005). Measuring the off-axis angle and the rotational movements of phonating sperm whales using a single hydrophone, *Journal of Acoustical Society of America.* 119: 4074–4082.

Laplanche, C., Adam, O., Lopatka, M. & Motsch, J.-F. (2006). Male sperm whale acoustic behavior observed from multipaths at a single hydrophone, *Journal of Acoustical Society of America.* 118(5): 2677–2687.

Mallat, S. (1989). A theory for multiresolution signal decomposition: The wavelet representation, *IEEE Transaction on Pattern Analysis and Machine Intelligence* 11: 674–693.

Marquardt, D. W. (1963). An algorithm for least-squares estimation of nonlinear parameters, *SIAM Journal on Applied Mathematics* 11(2): 431–441.

Morrissey, R., Ward, J., DiMarzio, N., Jarvisa, S., & Moretti, D. (2006). Passive acoustics detection and localization of sperm whales in the tongue of the ocean, *Applied Acoustics* 62: 1091–1105.

Nosal, E. & Frazer, L. (2006). Delays between direct and reflected arrivals used to track a single sperm whale, *Applied Acoustics* 62: 1187–1201.

White, P., Leighton, T., Finfer, D., Powles, C. & Baumann, O. (2006). Localisation of sperm whales using bottom-mounted sensors, *Applied Acoustics* 62: 1074–1090.

[1] H. Glotin, P. Giraudet, F. Caudal at Inst. Nat. de la Propriété Intellectuelle, nb 07/06162, (2007).

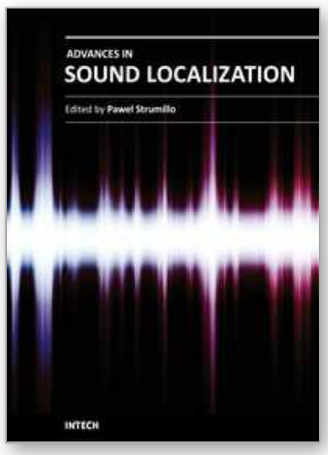

Advances in Sound Localization
Edited by Dr. Pawel Strumillo

ISBN 978-953-307-224-1
Hard cover, 590 pages
Publisher InTech
Published online 11, April, 2011
Published in print edition April, 2011

Sound source localization is an important research field that has attracted researchers' efforts from many technical and biomedical sciences. Sound source localization (SSL) is defined as the determination of the direction from a receiver, but also includes the distance from it. Because of the wave nature of sound propagation, phenomena such as refraction, diffraction, diffusion, reflection, reverberation and interference occur. The wide spectrum of sound frequencies that range from infrasounds through acoustic sounds to ultrasounds, also introduces difficulties, as different spectrum components have different penetration properties through the medium. Consequently, SSL is a complex computation problem and development of robust sound localization techniques calls for different approaches, including multisensor schemes, null-steering beamforming and time-difference arrival techniques. The book offers a rich source of valuable material on advances on SSL techniques and their applications that should appeal to researches representing diverse engineering and scientific disciplines.

How to reference
In order to correctly reference this scholarly work, feel free to copy and paste the following:

Frédéric Bénard, Hervé Glotin and Pascale Giraudet (2011). Highly Defined Whale Group Tracking by Passive Acoustic Stochastic Matched Filter, Advances in Sound Localization, Dr. Pawel Strumillo (Ed.), ISBN: 978-953-307-224-1, InTech, Available from: http://www.intechopen.com/books/advances-in-sound-localization/highly-defined-whale-group-tracking-by-passive-acoustic-stochastic-matched-filter

INTECH
open science | open minds

InTech Europe
University Campus STeP Ri
Slavka Krautzeka 83/A
51000 Rijeka, Croatia
Phone: +385 (51) 770 447
Fax: +385 (51) 686 166
www.intechopen.com

InTech China
Unit 405, Office Block, Hotel Equatorial Shanghai
No.65, Yan An Road (West), Shanghai, 200040, China
中国上海市延安西路65号上海国际贵都大饭店办公楼405单元
Phone: +86-21-62489820
Fax: +86-21-62489821

IntechOpen